

Clay Materials for Ceramics Application from N'Djamena in the Chad Republic: Mineralogical, Physicochemical and Microstructural Characterization

Ndjolba Madjihingam¹, Djoda Pagore¹, Jacques Richard Mache^{2*}, Bebbata Warabi¹, Bertin Pagna Kagonbe³, Patrick Mountapmbeme Kouotou^{1,4*}

¹Department of Civil Engineering, National Advanced School of Engineering, University of Maroua, Maroua, Cameroon

²Department of Mining Engineering, School of Geology and Mining Engineering, University of Ngaoundere, Meiganga, Cameroon

³Local Materials Authority Promotion (MIPROMALO), Yaoundé, Cameroon

⁴Department of Environmental Sciences, Advanced School of Agriculture, Forestry, Water and Environment, University of Ebolowa, Ebolowa, Cameroon

Email: *mkpatrick1982@gmail.com, *jamache@yahoo.fr

How to cite this paper: Madjihingam, N., Pagore, D., Mache, J.R., Warabi, B., Kagonbe, B.P. and Kouotou, P.M. (2024) Clay Materials for Ceramics Application from N'Djamena in the Chad Republic: Mineralogical, Physicochemical and Microstructural Characterization. *Journal of Materials Science and Chemical Engineering*, 12, 31-48.

<https://doi.org/10.4236/msce.2024.122003>

Received: January 10, 2024

Accepted: February 18, 2024

Published: February 21, 2024

Copyright © 2024 by author(s) and Scientific Research Publishing Inc.

This work is licensed under the Creative

Commons Attribution International

License (CC BY 4.0).

<http://creativecommons.org/licenses/by/4.0/>



Open Access

Abstract

Herein, we report some characteristics of the clayey materials (CMs) collected from Kaliwa (C1), Kabé (C2) and Malo (C3) district in N'Djamena (Chad). Three samples were characterized applying XRF, XRD, FTIR, SEM. In addition, TGA/DSC were performed to control decomposition/mass loss and show phase transitions respectively of CMs. Geochemical analysis by XRF reveals the following minerals composition: SiO₂ (~57% - 66%), Al₂O₃ (~13% - 15%), Fe₂O₃ (~6% - 10%), TiO₂ (~1% - 2%) were the predominant oxides with a reduced proportion in C1, and (~7%) of fluxing agents (K₂O, CaO, Na₂O). Negligible and trace of MgO (~1%) and P₂O₅ was noted. The mineralogical composition by XRD shows that, C1, C2 and C3 display close mineralogy with: Quartz (~50%), feldspar (~20%) as non-clay minerals, whereas clays minerals were mostly kaolinite (~15%), illite (~5%) and smectite (~10%). FTIR analysis exhibits almost seemingly similar absorption bands characteristic of hydroxyls elongation, OH valence vibration of Kaolinite and stretching vibration of some Metal-Oxygen bond. SEM micrographs of the samples exhibit microstructure reformed by inter-aggregates particles with porous cavities. TGA/DSC confirm the existence of quartz (570°C to 870°C), carbonates (600°C - 760°C), kaolinite (569°C - 988°C), illite (566°C - 966°C), MgO (410°C - 720°C) and smectite (650°C - 900°C). The overall characterization indicates that, these clayey soils exhibit good properties for ceramic

application.

Keywords

Clay Soils, Characterization, Mineralogy, Physicochemical Properties, Ceramic Application

1. Introduction

Clays materials (CMs), are well dispersed around the world and are widely employed in the manufacture and several structural products including ceramics products [1] [2]. Dried CMs is granular with a hydrophilic property that favour their plastic character upon contact with water, making them to be an easily malleable material. [2]. CMs are essentially composed of fine particles size generally constitute of several minerals including silica, alumina or magnesia or both and water, associated with minor constituents such as oxides from iron (Fe), potassium (K), calcium (Ca), magnesium (Mg), titanium (Ti) and sodium (Na) and other companion minerals such as quartz and feldspars, etc [3]. Generally, the type of the ceramic product to be manufactured strongly influenced by the structural composition and physicochemical characteristics of the raw materials used in the manufacturing process [4].

N'Djamena (Chad republic) in general and particularly Kaliwa (C1), Kabé (C2) and Malo (C3) district dispose of high proportion, clay materials exploited for several traditional utilisation, especially as traditional fired bricks and blocks and pottery. However, application of these raw materials as building materials has weaknesses in terms of tensile and compressive strength [5], as well as deterioration due to rapid erosion when exposed to water [6]. In addition to these defects due to their intrinsic characteristics, the use of clays in sustainable construction in the Logone valley is a real challenge because of the structural failures caused by compression/tension and swelling/shrinkage effects [7] [8] [9]. Moreover, the temperature gradients coupled with the above-mentioned swelling/shrinkage phenomenon experienced by these compressed clay bricks of Kaliwa, Kabé and Malo are responsible of the particle's motion and the formation of pores, which leads to the appearance of cracks in all directions [10]. In contrast, traditional pottery is booming for a variety of purposes. The practice is intimately linked to the way of life of the people of N'Djamena. In the Kaliwa (C1), Kabé (C2) and Malo (C3) district, pottery is considered a utensil for cooking food and the traditional beer. The ceramic production activity is mostly carried out by women in traditional processing manner, which do not necessarily take into consideration mineralogical, physicochemical and microstructural properties as well as relevant procedure including drying, mixing and fashioning. Therefore, the locally produced fired blocks, bricks and pottery are mostly of poor standard exhibiting low durability and mechanical resistance.

Clay materials in Chad Republic are unknown, underutilized, and scientifically unstudied. As consequence, their unknown structural and physico-chemical properties strongly limit their traditional application in ceramics products. To date, there is no systematic reported study on such intensive use materials available in the literature. The aim of this work was to study the suitability of the abundant clay materials sourced from three districts of N'Djamena in Chad Republic in ceramic making and to pave the ways for industrial applications.

Clay materials were collected from Kaliwa, (C1), Kabé (C2) and Malo (C3) districts in N'djamena and systematically studied by classical analytical techniques. The geochemistry analysis using X-ray fluorescence spectroscopy (XRF) was performed in order to examine the distribution of chemical elements and ascertain the composition of major mineral elements in CMs. X-ray diffraction (XRD) enabled to study the mineralogical characterization of CM materials and identify the type and structure of crystallized materials [11] [12]. Furthermore, Fourier transform infrared (FTIR) spectroscopy was performed additionally to the XRD to identify functional groups at the surface of the CMs materials [13] [14]. In addition, Scanning Electron Microscopy (SEM) was performed to analyse the shape and microstructure of the CMs surfaces [15]. Moreover, Thermogravimetric analysis was investigated to detect important changes and alterations such as dehydration, dihydroxylation and recrystallization occurring in the materials during heating process [16]. Finally, the suitability of the studied CMs for ceramics application was performed based on well-known empirical diagrams.

2. Materials and Methods

2.1. Sampling Methods and Geographical Coordinates

Clay materials analysed (Figure 1) in the present work were collected from three distinct localities (Kaliwa (C1), Kabé (C2) and Malo (C3)) in the commune of N'Djamena in the Chad Republic as displayed on the map of Figure 2.

2.2. Methods

2.2.1. Physical Analysis

Particle size distribution: the particle size dissemination was studied using wet sieving (fraction $\geq 80 \mu\text{m}$) and sedimentation through gravity (fraction $< 80 \mu\text{m}$).



Figure 1. Samples as collected from Kaliwa (C1), Kabé (C2) and Malo (C3).

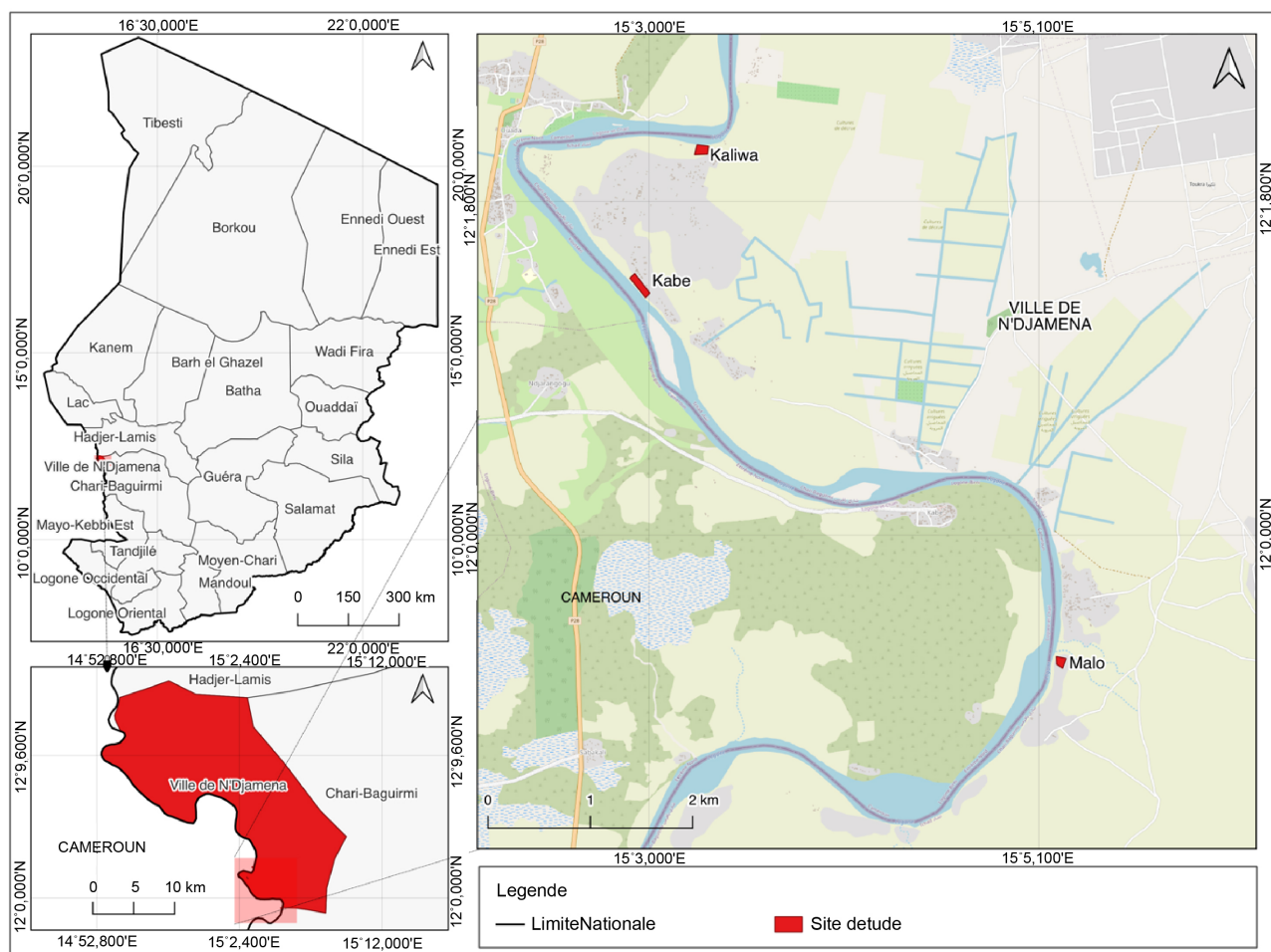


Figure 2. Map location of sampling area.

Atterberg limits: the Casagrande technic was employed to determine parameters such as the liquid (W_l) and plasticity (W_p) limit as well as the index of plasticity (IP). These analyses were performed in agreement with their respective well-established norm including: NFP norm, NF P 94-056 and NF P 94-057.

2.2.2. Geochemistry Study by X-Ray Fluorescence Spectroscopy (XRF)

X-ray fluorescence spectroscopy (XRF) method was employed to determine the chemical composition. The experiment was performed using a Philips XRFSPW 1404 spectrometer at the Cameroon cement plant (Cimencam) of Figuil in Cameroon (Lafarge group).

2.2.3. Structure Analysis by X-Ray Diffraction (XRD) Analysis

In order to ascertain the structural information of the studied sample powders, XRD analysis was carried out using a diffractometer from Bruker (Cu anticathode $K\alpha_1$ ($\lambda = 1.5406 \text{ \AA}$), $\lambda = 1,5418 \text{ \AA}$, $V = 40 \text{ kV}$, $I = 30 \text{ mA}$). The analysis was performed over $2^\circ < 2\theta < 70^\circ$ (Step size: 0.02° and time per step 2s), in the Bragg-Brentano θ/θ configuration. Peak intensities of XRD patterns used for both qualitative and semi-quantitative was approximate [17] [18].

2.2.4. Fourier Transform Infrared (FT-IR) Spectroscopy

The chemical bonds and clay materials surface functional groups were determined by FT-IR. The experiment was performed on a Bruker Alpha-P spectrometer (Thermo Electron) in absorbance mode. The spectra were recorded within the spectral range (250 - 4000) cm^{-1} with a resolution of 4 cm^{-1} .

2.2.5. Thermal Analysis Thermogravimetric Analysis (TGA) and Differential Scanning Calorimetry (DSC)

TGA and DSC experiment was investigated to bring out the transition signals correlated to mass losses and/or phase changes. The analysis was performed on a SetaramLABevo TG-DSC 1600°C device, running under Argon flow. Starting from the room temperature, samples were heated up to 1200°C within a ramp of 10 to 40°C·min⁻¹. The DSC survey was run in an air flow, with Al₂O₃ crucibles.

2.2.6. Scanning Electron Microscopy (SEM)

The morphology at the microscopic scale was analysed on a Philips microscope model XL30 (Liege, Belgium) with high-voltage accelerated electron beams. The CM samples were regularly disposed on a sample supporter and then installed in a SEM yard maintained in a vacuum of 5×10^{-2} Pa.

3. Results

3.1. Physical Analysis

Sample clay materials C1, C2 and C3 consist of 42.9% - 63.1% sand, 614.7% - 28.2% silt and 22.2% - 28.9% clay, while sample C1 and C2 exhibits a high percentage of sand than C3. The elevated content percentage of sand in these samples enable us to attest that, the studied materials is a clayey sand exhibiting homogeneous and dispersed particle size. The particle size distribution of individual studied CMs and the ATTERBERG limit test details are presented in **Table 1**. The CMs exhibit a plasticity index in between 27 and 31.0, that is: 31.0%,

Table 1. Physical properties of studied clay samples from Kaliwa (C1), Kabe (C2) and Mallo (C3).

	Studied clay samples		
	C1	C2	C3
Particle size distribution (%)			
Clay: (<0.002 mm)	22.2	23.8	28.9
Silt: (0.002 - 0.02 mm)	14.7	24.4	28.2
Sand: (0.02 - 2 mm)	63.1	51.8	42.9
Gravel: (>2 mm)	0.0	0.0	0.0
Atterberg limits (%)			
Liquid limit (WL)	63.4	60.7	57.6
Plastic limit (WP)	32.4	32.7	30.4
Plastic index (IP)	31.0	28.0	27.2

28.0% and 27.2% respectively C1, C2 and C3 samples. The data from **Table 1** were used to plot the Holtz and Kovacs diagrams presented in **Figure 3**, which indicate that, that sample CMs samples C1, C2 and C3 exhibits a kaolinitic character and are highly plastic.

In addition, CMs pottery and extrusion brick-making potential was studied. The position of the CMs in the diagram of Bain and Highley is presented in **Figure 4**. From **Figure 4**, it is obvious that, the studied CMs exhibits good properties for pottery and acceptable for extrusion brick-making. However, the chemical composition, the nature of the mineralogical phases, the size of the grains and the firing parameters are the main factors which influence the quality of pottery and extrusion brick-making. Furthermore, mixing and drying of the raw material is important in the process of producing pottery objects.

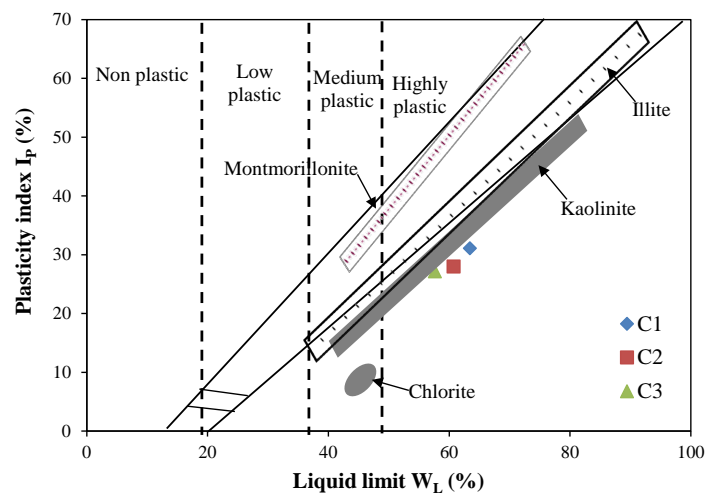


Figure 3. Diagram of Holtz and Kovacs [19] showing the kaolinitic character of C1, C2 and C3.

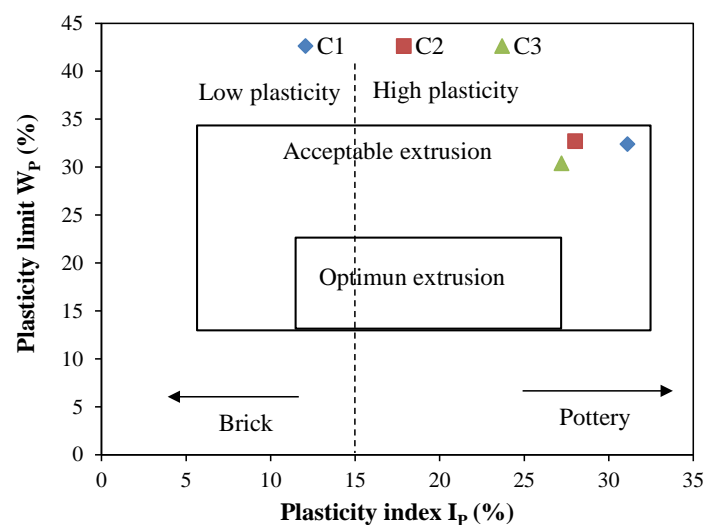


Figure 4. Diagram of Bain and Highley [20] showing samples good for pottery, samples acceptable for extrusion brick-making.

3.2. Geochemistry of the Samples (C1, C2 and C3) by XRF

The geochemistry study was carried out on C1, C2 and C3. The chemical elements distribution and major mineral elements in the CMs are displayed in **Table 2**. From **Table 2**, it obvious that, the overall samples exhibit the same mineral composition but with variable proposition.

The geochemical analysis of Kaliwa site (C1) revealed that the major elements are silica (SiO_2 : 57.28%), alumina (Al_2O_3 : 14.36%) and iron oxides (Fe_2O_3 : 9.23%). SiO_2 is the dominant mineral compared to the other minerals. The presence of alkaline and alkaline earths metals is remarkable: potassium (K_2O : 3.64%), titanium (TiO_2 : 1.40%), sodium oxide (Na_2O : 1.08%), calcium oxide (CaO : 1.05%) and magnesium oxide (MgO : 0.73%). Other constituents such as manganese oxide (MnO : 0.17%) and Phosphorus oxide (P_2O_5 : 0.14%), although present, are negligible. The loss on fire for C1 is relatively low (~10.92%).

As far as the sample (C2) from Kabé district site is concerned, the major minerals are composed of silica (SiO_2 : 65.81%), alumina (Al_2O_3 : 12.29%) and iron oxides (Fe_2O_3 : 6.16%). The proportion of silica with 65.81% highest dominant mineral compared to other minerals in respective samples (**Table 1**), while Fe_2O_3 with only 6.16% remain the lowest. Alkaline and alkaline earth metals are essentially the same but with a slight difference in term of concentration. K_2O (4.10%), TiO_2 (1.09%), Na_2O (1.26%), CaO (1.31%) and MgO (0.75%) are present, while

Table 2. Chemical composition of studied clay samples from Kaliwa (C1), Kabe (C2) and Mallo (C3).

	Studied clay samples		
	C1	C2	C3
Chemical composition (wt.%)			
SiO_2	57.28	65.81	58.70
Al_2O_3	14.36	12.29	14.40
Fe_2O_3	9.23	6.16	7.27
K_2O	3.64	4.10	3.67
MgO	0.73	0.75	0.91
TiO_2	1.40	1.09	1.40
P_2O_5	0.14	0.09	0.12
CaO	1.05	1.31	2.61
Na_2O	1.08	1.26	1.04
MnO	0.17	0.11	0.07
L.O.I	10.92	7.03	9.81
Total	100	100	100
$\text{SiO}_2/\text{Al}_2\text{O}_3$	3.99	5.35	4.08
$\text{CaO} + \text{MgO} + \text{K}_2\text{O} + \text{Na}_2\text{O}$	6.5	7.42	8.23
CIA	71.33	64.82	62.30

Mn_2O_3 (0.11%) and P_2O_5 (0.11) are still negligible. The loss on fire is 0~7.03% and is lower for Kabé site. Analogously to the Karewa (C1) and Kabé (C2) sites, the Malo (C3) site results present the same constituents for which the comparative proportions are almost similar (see **Table 2**).

The geochemical analysis presents a chemical composition of the materials that constitute the CMs studied. Major elements and fire loss are presented in **Table 2**. It appears that Kabé site contains more silica than others. The soils of Malo and Karewa display almost identical alumina values. Iron is higher in Karewa soil. Alkalis and alkaline earths show mixed results. The fire loss is lower in Kaliwa and even lowest in Kabé.

The geochemistry analysis gives a precise idea of the geochemical composition of the clay formations on the Kaliwa, Kabé and Malo sites. Indeed, these samples present similar geochemical characteristics from one site to another. According to the results obtained, variations in the contents of major elements are relatively high in the overall samples in the present investigation. The main oxides listed in order of their content's importance are SiO_2 , Al_2O_3 , Fe_2O_3 , K_2O , CaO , MgO , TiO_2 and SiO_2 varying from 57.28 to 65.81% in the studied sites. The highest rate is from the sample collected from Malo district (C2), followed by that from Kabé district (C3) and finally sample from the Kaliwa district (C1).

The XRF results suggested in general that, the studied CMs are essentially composed of alumina silicate with an excess of quartz-forming silica. The obtained results are in accordance with those obtained by Mache *et al.*, and Kagonbé *et al.* [4] [21], who reported that, the CMs from the Sudano-Sahelian areas are mainly composed of silica. However, the occurrence of Al_2O_3 in the materials studied depend on the existence of CMs such as kaolinite, while the presence of kaolinite in these minerals highlights this geochemical process called mono-sialization followed by bis-sialization. The presence of Fe_2O_3 at a relatively high concentration suggests the presence of hematite phase in good agreement with the literature [4]. CaO and MgO are quantitatively low in the samples studied due the low content of carbonate minerals observed in most of the samples. The potassium and sodium oxide contents present in the clay raw material could probably be attributed to the presence of illite [22].

The Loss on Ignition results is in the range of 7 to 11% in overall samples. The highest rate of loss on ignition is obtained for sample from Kaliwa. These CMs would have undergone dehydroxylation reactions, combustion of organic matter and decomposition of CMs carbonates [23]. In addition, other melting minerals like illite and smectite are suggested to be present in agreement with earlier results in the literature [24].

3.3. Mineralogical Composition by X-Ray Diffraction Analysis

The XRD patterns of the CMs samples, displaying variable peaks intensities are presented in **Figure 5**. **Figure 5** exhibits a perfect similarity between the XRD patterns of the entire studied samples with a basal reflection at higher ($\sim 14.66 \text{ \AA}$)

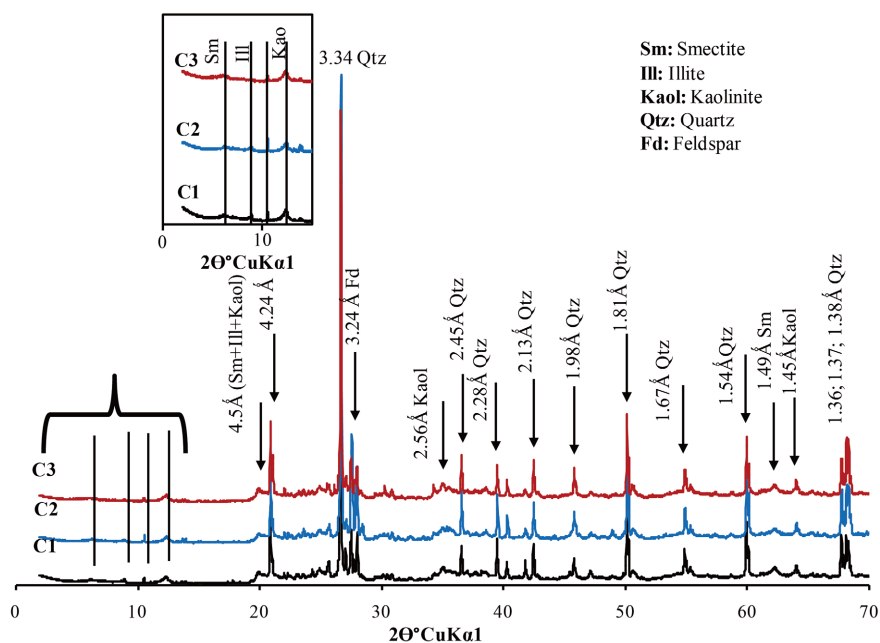


Figure 5. X-ray diffraction patterns of clay soils from Kaliwa (C1), Kabé (C2) and Malo (C3).

and lower (~ 1.49 Å) diffraction angle, attesting of the occurrence of smectite. The weak peaks recorded at ~ 10.22 Å confirm the presence illite and those at ~ 7.31 , ~ 2.56 and at ~ 1.45 Å are characteristics of kaolinite phase. The peaks characteristic of quartz minerals appears at 3.34 Å and 4.24 Å, while the signal corresponding to the feldspars is detected consecutively in the diffraction angle located at 3.77 and at 3.46 Å respectively. The remaining shrill peaks are essentially linked to presence of quartz. The XRD analysis revealed that, major crystalline phases detected are mainly made up of smectite, Illite ($K_2O \cdot 2H_2O$, $2Al_2(Si_3Al)O_{10}(OH)$), kaolinite ($Si_2O_5Al_2(OH)_4$), quartz (SiO_2) and Felds paths ($Ba, Ca, Na, K, NH_4)(Al, B, Si)_4O_8$.

The XRD results for all samples indicate that smectite has been characterized as dioctahedral smectite, confirmed by the presence of kaolinite at ~ 7.31 Å mineral generally phase associated with smectite. In the overall samples, quartz (~ 3.34 Å) and K-feldspars (~ 2.90 - ~ 3.77 Å) coexist as accessory minerals. The mineralogical composition of the CMs in this study reveals that, the samples possess high content of Quartz (50%) followed by feldspar (20%), kaolinite (15%), smectite (10%) and illite (5%). The observed free silica in the CMs is due to the detected quartz as it is confirmed by the calculation of the SiO_2/Al_2O_3 ratio. This quartz content with the contribution of kaolinite are definitely an asset in the compressed CMs bricks formulation.

The peaks shape characteristic of the as-studied minerals account of their crystallized nature. The intensity of peaks characteristics to quartz attest on their preponderance throughout the mineralogical sphere. The variations observed in the mineralogy composition of the studied CMs account on the difference on their erodibility character. Indeed, soils whose mineralogy is impacted by the

presence of 2:1 type clay such as smectite and kaolinite are sensitive to runoff and erosion once in contact with water [25] [26]. This physical character will have an impact on the mechanical properties of the as-studied CMs materials.

3.4. Surface Chemicals Bonds and Functional Groups Analysis by FTIR

The infrared spectra of the overall samples are almost similar and include the presence several absorption bands as depicted in **Figure 6(a)**, **Figure 6(b)**. The adsorption bands ranging from 3750 to 3500 cm^{-1} are characteristic of the elongation of the hydroxyl groups; while those at ~ 3696 , ~ 3642 and ~ 3620 cm^{-1} are characteristic of kaolinite phase [25] [26]. The observed two significant vibration bands suggest that, the kaolinite phases present in the CMs exhibits a disordered structure [27]. An elongation vibration bands ranging from ~ 3642 to ~ 3696 cm^{-1} , are attributed to inter-layer hydroxyl groups. It is worth to mention that, the intensities and positions of those hydroxyl groups are usually sensitive to the intercalation of organic molecules. The Al-OH and Al-O-Si deformation vibration bands appear from ~ 905 cm^{-1} in perfect agreement with the literature. [28] [29] while the shoulders at ~ 675 cm^{-1} can be assigned to the presence of quartz [29]. The vibration bands around ~ 3420 and ~ 3460 cm^{-1} can be attributed to the Si-O vibrations, while that located at ~ 525 and ~ 765 cm^{-1} are assigned to different vibration modes of Si-O-Al bonds (where Al is tetra coordinated) in kaolinite. The band at 905 cm^{-1} characteristic of the δ Al-OH group deformation of [30], will disappear to give way to a wide band up to 995 cm^{-1} , belonging to the Si-O-Si bonds of the kaolinite. This modification would be due to the formation of an amorphous structure as already noticed with the XRD analysis (**Figure 3**).

FTIR results are in good agreement with XRD data and therefore, confirm the presence of Quartz, Kaolinite and Illite in the CMs studied. The Si-O-Si bonds of kaolinite are also identified at 645 cm^{-1} [31] [32]. The deformation vibrations of

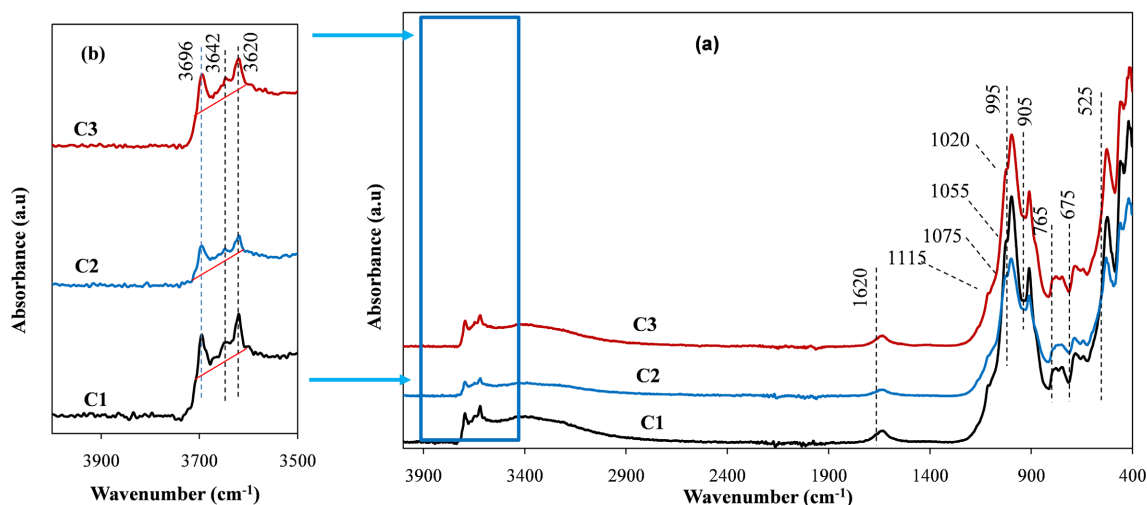


Figure 6. (a) Complete FTIR Spectra of Clay soils from Kaliwa (C1), Kabé (C2), Malo (C3), (b) OH stretching domain.

the Al-O bonds appear at 690 cm^{-1} [33]. Quartz and feldspars absorb very little radiation in the visible or near-IR ranges, hence their sober appearance [34]. The intensity of the peak broad band at 750.57 cm^{-1} corroborates with the abundance of Quartz [35] in line with XRD results.

3.5. Thermogravimetric and Differential Scanning Calorimetry (TGA & DSC)

Thermogravimetric and differential analyzes (TGA/DSC) for all samples were carried out and the resulting curves are presented on **Figure 7** and **Figure 8**. **Figure 7** presents the heat flow variation with temperatures for the three samples. From the **Figure 7** two prominent endothermic peaks located between the temperature of 0 to 260°C and 400 to 600°C as well as another barely perceptible exothermic peak in between 900 and 1000°C were observed for the overall samples. The observed picks can be assigned to the water loss, the decomposition of hydroxides and organic matter and finally the quartz transformation and the loss into carbonates. The first peak at 87°C corresponds to the water hygroscopic departure from the illite sheets [36] [37] [38]. The second endothermic picks at ~ 482 , 488, 494 and 553°C for sample C1, C2 and C3 respectively followed by mass losses are due to hydroxylation (OH) of kaolinite (transformation into metakaolinite and smectite).

The exothermic peaks of thermograms observed around 561°C , 545°C and 557°C respectively for the three samples C1 C2 C3, illustrate the hydroxylation of illite and smectite (**Figure 7**). The quartz content of the three samples could not be compared due to the overlapping peaks similarity from different minerals. Quartz is identified here by its progressive disintegration in the temperature range of 927 to 948°C , with a shift in its content around 1100°C ; although the

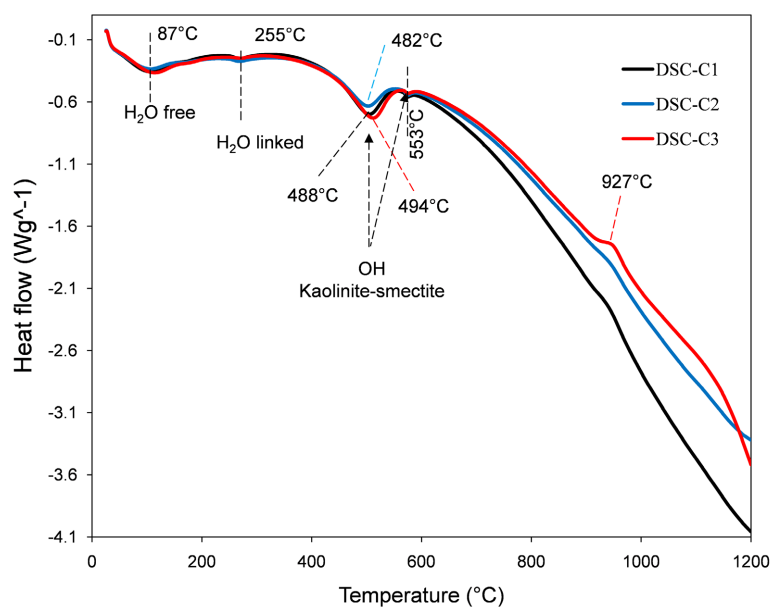


Figure 7. DSC curves of studied samples (C1, C2 and C3).

effective temperatures at which the carbonate decomposes can sometimes fluctuate [38] [39]. This exothermic phenomenon is related to the metakaolinite structural reorganization.

The three curves in **Figure 8** highlight the mass losses as a function of the peaks observed on **Figure 4**. From the TGA curve on **Figure 8**, the mass loss of 1.33, 1.18 and 1.29% was observed for C1, C2 and C3 respectively. The second endothermic peaks between 453 and 550°C (C1), between 450 and 530°C (C2) and between 486 and 546°C (C3) following the mass losses 6.1, 4.22 and 5.86% respectively are due to hydroxylation kaolinite and their transformation into

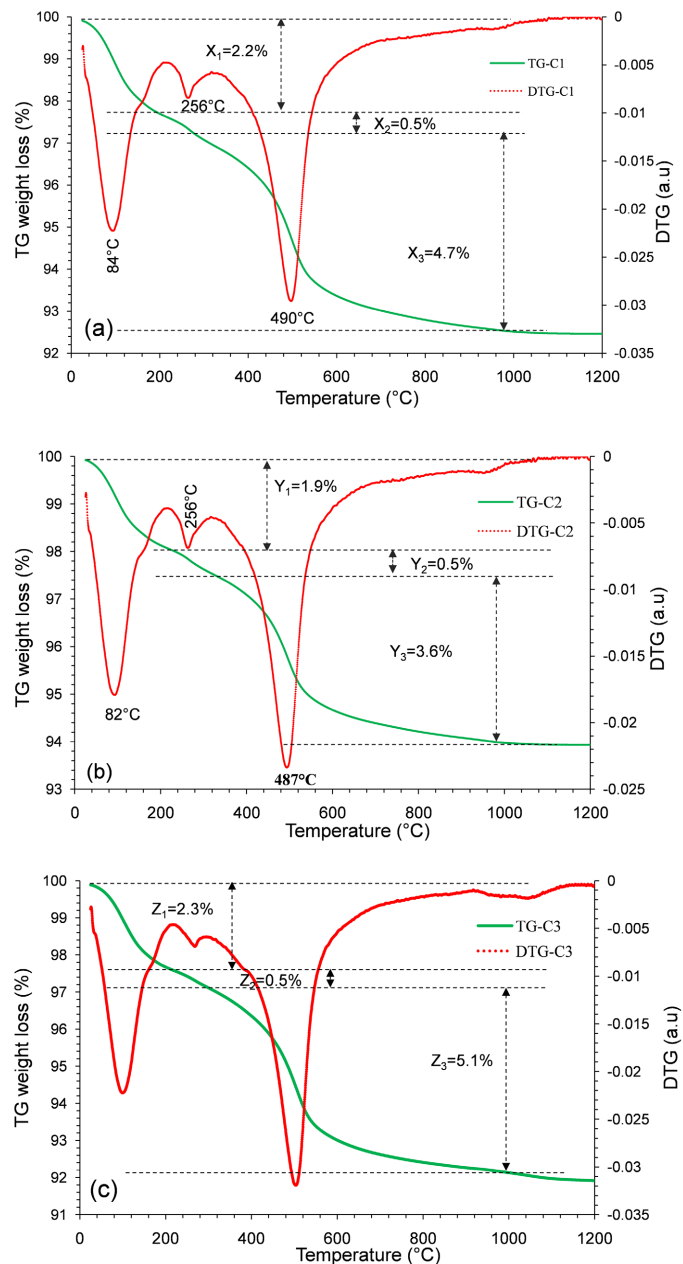


Figure 8. TG and DTG curves of clay soils from a-Kaliwa (C1), b-Kabé and (C2) from c-Malo (C3).

metakaolinite. The overall CMs exhibits characteristic of water constituent elimination, resulting from the release of structure dihydroxylation [39] [40] [41].

3.6. Surface Morphology Inspection by SEM

Scanning electron microscopy is a useful tool used to observe the texture and microstructure of the clay soil in the sample and characterize the mineralogical assemblages. The morphological configuration of soil samples C1 from Kaliwa C2 from Kabé and C3 from Malo was analyzed and present **Figure 9**. Their textures display clay particles with various heterogeneous shapes surrounded with porous and open cavities. Several stacked observed on top of each other in adjacent crystals to form clusters were detected. The irregularity of the particle sizes is characteristic of the illite. a great number of clusters scattered on each samples micrograph, suggesting the presence of Al, Si, Mg, Fe, Na, Ca, K, Ti and O chemicals constituents present in the entire CMs samples in the form of oxides (Al_2O_3 , SiO_2 , Fe_2O_3 , MgO , Na_2O , CaO , K_2O and TiO_2 already observed above by XRF and XRD analysis. The high content of SiO_2 , Al_2O_3 and FeO in some grains confirms the presence of kaolinite. The microstructural analysis of the set of three samples with SEM revealed the presence of smectites in the form of clusters in superimposed sheets where undulations are perceptible [42] [43].

4. Suitability for Ceramic Products

The mineralogical compositions, physicochemical properties and thermal behavior of the studied CMs were almost similar. The ratio of $\text{SiO}_2/\text{Al}_2\text{O}_3$ is range between 4.0 to 5.4 and the cumulative percentage of $6.5\% < \text{CaO} + \text{MgO} + \text{K}_2\text{O} + \text{Na}_2\text{O} < 8.2\%$ are very important to elaborate a ceramic product with these raw clay materials. The evaluation of the suitability of the studied raw materials base on empirical diagram of Winkler (1954) (see **Figure 10**) indicated that, the three clay samples are suitable of grains fractions for roofing tiles lightweight bricks and thin-walled.

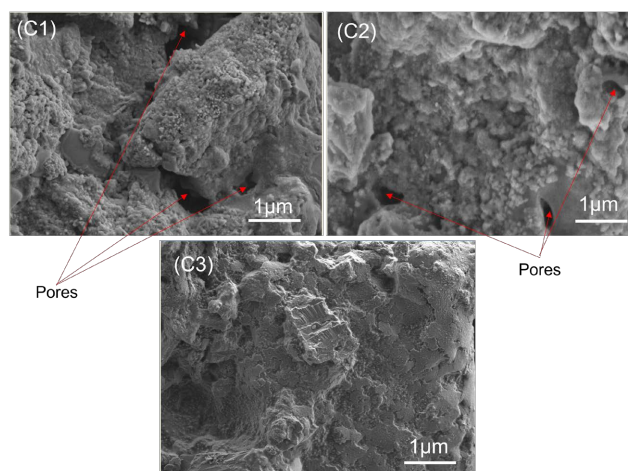


Figure 9. SEM micrographs of clay soils from Kaliwa (C1), Kabé (C2) and Malo (C3).

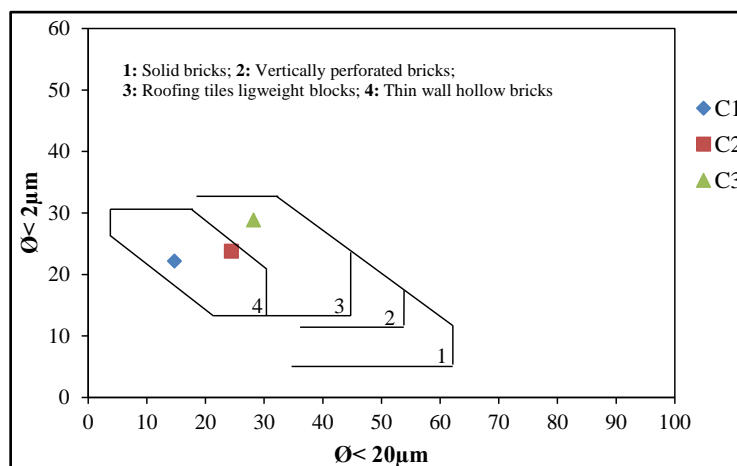


Figure 10. Ceramic product suitability evaluation of CMs base on empirical diagrams. Diagram of Winkler (1954) in [44] showing suitable mixtures of grains fractions for roofing tiles lightweight bricks (3) and thin-walled hollow bricks (4).

The CMs in the present work are characterized by a high plasticity index ($I_p > 25$), responsible to their plastic character with regard to their texture. They are all mineralogically composed of kaolinite-smectite-illite as clay minerals. The observed non-clay minerals like quartz-Feldspar, presents a certain similarity in terms of chemical composition in major oxides and almost identical thermal behavior for three clay materials. The overall studied properties of the CMs in this investigation allows us to specify their probable application including fired extruded bricks and pottery. Taking in account the availability of the raw materials (CMs), Kaliwa, Kabé and Malo, the cost of pottery will be drastically reduced.

5. Conclusion

This investigation has enabled us to identify mineralogical, physicochemical and microstructural analyzes characteristic clayey materials originating from the Kaliwa, Kabé and Malo district (N'Djamena, Chad). Both geochemistry and mineralogical indicated that the three sets of samples contain essentially the same chemical elements with almost identical proportions including: silica SiO_2 (57.28% - 65.81%), alumina Al_2O_3 (12.29% - 14.40%) and iron oxide Fe_2O_3 (6.16% - 9.23%) as major constituents. Alkalines and alkaline earth such as potassium K_2O (3.64% - 4.10%), titanium TiO_2 (1.09% - 1.40%), sodium Na_2O (1.08% - 1.26%), calcium CaO (1.05% - 2.61%), magnesium MgO (0.73% - 0.91%) are negligible. The low values of mass loss on ignition (10.92%) for these soils are confirmed by thermal analyses. XRD revealed that the three sites have similar mineralogy; quartz (~50%) and feldspar (~20%) being non-clay minerals, while clay minerals are mainly kaolinite (~15%), illite (~5%), and smectite (~10%). FTIR confirmed the presence of these oxides from peaks which show the vibrational movement of said oxides. SEM texture showed clay particles ex-

hibiting heterogeneous shapes with porous cavities and faults corresponding to inter-aggregates. The DTA/TGA highlighted transformation phases of these ores with the temperature variation. The overall results indicate that, these CMs exhibit good properties for ceramic application. This work offers a novel raw material for an effective ceramic application.

Acknowledgements

Prof. Désiré Tsozué from the University of Maroua, Faculty of Sciences at the Department of Geological Sciences is strongly deeply acknowledged to have facilitated some analysis in the present study.

Conflicts of Interest

The authors declare no conflicts of interest regarding the publication of this paper.

References

- [1] Murray, H. (2007) Applied Clay Mineralogy: Occurrences, Processing and Applications of Kaolins, Bentonites, Palygorskitesepiolite and Common Clays. *Developments in Clay Science*, Elsevier, Amsterdam, 180. [https://doi.org/10.1016/S1572-4352\(06\)02008-3](https://doi.org/10.1016/S1572-4352(06)02008-3)
- [2] Tsozué, D., NzeukouNzeugang, A., Maché, J.R., Loweh, S. and Fagel, N. (2017) Mineralogical, Physico-Chemical and Technological Characterization of Clays from Maroua (Far-North, Cameroon) for Use in Ceramic Bricks Production. *Journal of Building Engineering*, **11**, 17-24. <https://doi.org/10.1016/j.jobbe.2017.03.008>
- [3] Mukherjee, S. (2013) The Science of Clays: Applications in Industry, Engineering and Environment. Springer, New Delhi.
- [4] Kagonbé, B.P., Tsozué, D., Nzeukou, A.N. and Ngos III, S. (2021) Mineralogical, Physico-Chemical and Ceramic Properties of Clay Materials from Sekandé and Gashiga (North, Cameroon) and Their Suitability in Earthenware Production. *Helion*, **7**, e07608. <https://doi.org/10.1016/j.helion.2021.e07608>
- [5] Amer, A.A., Mattheus, F.A.G. and Ghazi, A.A. (2006) Geology, Classification, and Distribution of Expansive Soils and Rocks: A Case Study from the Arabian Gulf Expansive Soils. CRC Press, Boca Raton.
- [6] Zhang, C., Bai, Q., Han, P., Wang, L., Wang, X. and Wang, F. (2023) Strength Weakening and Its Micromechanism in Water-Rock Interaction, a Short Review in Laboratory Tests. *International Journal of Coal Science & Technology*, **10**, Article No. 10. <https://doi.org/10.1007/s40789-023-00569-6>
- [7] Nshimiyimana, P., Nathalie Fagel, N., Messan, A., Wetschondo, D.O. and Courard, L. (2020) Physico-Chemical and Mineralogical Characterization of Clay Materials Suitable for Production of Stabilized Compressed Earth Blocks. *Construction and Building Materials*, **241**, Article ID: 118097. <https://doi.org/10.1016/j.conbuildmat.2020.118097>
- [8] He, I.L., Atheba, G.P., Allou, N.B., Drogui, P., EI Khakani, M.A. and Gbassi, G.K. (2023) Physic, Chemical and Mineralogical Characterizations of Clays Used in the Making of Traditional Ceramics in the City of Katiola, Côte d'Ivoire. *Journal Minerals and Materials Characterization Engineering*, **11**, 81-91. <https://doi.org/10.4236/jmmce.2023.114008>

- [9] Ekpo, D.T., Agossou, Y.D., Agbelele, J. and Adjovi, E.C. (2023) Physical Characterization of Laterite for the Formulation of Structural Concrete. *Open Journal of Civil Engineering*, **13**, 411-426. <https://doi.org/10.4236/ojce.2023.133031>
- [10] Robin, V., Cuisinier, O., Masrouf, F. and Javad, A.A. (2014) Chemo-Mechanical Modelling of Lime Treated Soils. *Applied Clay Sciences*, **95**, 211-219. <https://doi.org/10.1016/j.clay.2014.04.015>
- [11] Kagonbé, B.P., Tsozué, D., Nzeukou, A.N. and Ngos III, S. (2021) Mineralogical, Geochemical and Physico-Chemical Characterization of Clay Raw Materials from Three Clay Deposits in Northern Cameroon. *Journal of Geoscience and Environment Protection*, **9**, 86-99. <https://doi.org/10.4236/gep.2021.96005>
- [12] Ural, N. (2021) The Significance of Scanning Electron Microscopy (SEM) Analysis on the Microstructure of Improved Clay: An Overview, *Open Geosciences*, **13**, 197-218. <https://doi.org/10.1515/geo-2020-0145>
- [13] Nguetnkam, J.P., Villiéras, F., Kamga, R., *et al.* (2014) Mineralogy and Geochemical Behaviour during Weathering of Greenstone Belt under Tropical Dry Conditions in the Extreme North Cameroon (Central Africa). *Geochemistry*, **74**, 185-193. <https://doi.org/10.1016/j.chemer.2013.06.007>
- [14] Saiyouri, N., Hicher, P.Y. and Tessier, D. (2000) Microstructural Approach and Transfer Water Modelling in Highly Compacted Unsaturated Swelling Clays. *Mechanics of Cohesive-Frictional Materials*, **5**, 41-60. [https://doi.org/10.1002/\(SICI\)1099-1484\(200001\)5:1<41::AID-CFM75>3.0.CO;2-N](https://doi.org/10.1002/(SICI)1099-1484(200001)5:1<41::AID-CFM75>3.0.CO;2-N)
- [15] Cases J.M., Lietard, O., Yvon, J. and Delon, J.F. (1982) Etude des propriétés cristalochimiques, morphologiques, superficielles de kaolinites désordonnées. *Bulletin de Minéralogie*, **5**, 439-456. <https://doi.org/10.3406/bulmi.1982.7566>
- [16] Jozanikohan, G., Sahabi, F., Norouzi, G.H. and Memarian, H. (2015) Thermal Analysis: A Complementary Method to Study the Shurijeh Clay Minerals. *International Journal of Mining & Geo-Engineering*, **49**, 33-45.
- [17] Cook, H.E., Johnson, P.D., Matti, J.C. and Zemmels, I. (1975) Methods of Sample Preparation and X-Ray Diffraction. Data Analysis, X-Ray Mineralogy Laboratory, Deep Sea Drilling Project, University of California, Riverside. Contribution No. 74-5, 999-1007. <https://doi.org/10.2973/dsdp.proc.28.app4.1975>
- [18] Fagel, N., Boski, T., Likhoshway, L. and Oberhaensli, H. (2003) Late Quaternary Clay Mineral Record in Central Lake Baikal (Academician Ridge, Siberia). *Palaeogeography, Palaeoclimatology, Palaeoecology*, **193**, 159-179. [https://doi.org/10.1016/S0031-0182\(02\)00633-8](https://doi.org/10.1016/S0031-0182(02)00633-8)
- [19] Holtz, R.D. and Kovacs, W.D. (1981) An Introduction to Geotechnical Engineering. Prentice Hall, Englewood Cliffs.
- [20] Bain, J.A. and Highley, D.E. (1978) Regional Appraisal of Clay Resources—A Challenge to the Clay Mineralogist. *Developments in Sedimentology*, **27**, 437-446. [https://doi.org/10.1016/S0070-4571\(08\)70741-6](https://doi.org/10.1016/S0070-4571(08)70741-6)
- [21] Mache, J.R., Signing, P., Mbey, J.A., Razfitianamaharavo, A., Njopwouo, D. and Fagel, N. (2015) Mineralogical and Physico-Chemical Characteristics of Cameroonian Smectitic Clays after Treatment with Weakly Sulfuric Acid. *Clay Minerals*, **50**, 649-661. <https://doi.org/10.1180/claymin.2015.050.5.08>
- [22] Mohammad, S.H., Shakor, P., Muhammad, J.H., Hasan, M.F. and Karakouzian, M. (2023) Sustainable Alternatives to Cement: Synthesizing Metakaolin-Based Geopolymer Concrete Using Nano-Silica. *Construction Materials*, **3**, 276-286. <https://doi.org/10.3390/constrmater3030018>
- [23] Baccour, H., Medhioub, M., Jamoussi, F., Mhiri, T. and Daoud, A. (2008) Minera-

- logical Evaluation and Industrial Applications of the Triassic Clay Deposits. *Southern Tunisia Materials Characterization*, **59**, 1613-1622. <https://doi.org/10.1016/j.matchar.2008.02.008>
- [24] Christidis, G. (2011) Industrial Clays. *European Mineralogical Union Notes in Mineralogy*, **9**, 341-414. <https://doi.org/10.1180/emu-notes.2010.emu9-9>
- [25] Nguetnkam, J.P. and Dultz, S. (2024) Clay Dispersion in Typical Soils of North Cameroon as a Function of pH an Electrolyte Concentration. *Land Degradation & Development*, **25**, 153-162. <https://doi.org/10.1002/ldr.1155>
- [26] Farmer V.C. (1974) The Infrared Spectra of Minerals. Mineralogical Society, London. <https://doi.org/10.1180/mono-4>
- [27] Frost, R.L. and Vassallo, A.M. (1996) The Dehydroxylation of the Kaolinite Clay Minerals Using Infrared Emission Spectroscopy. *Clays and Clay Minerals*, **44**, 635-651. <https://doi.org/10.1346/CCMN.1996.0440506>
- [28] Jakub, M., Adam, G. and Krzysztof, B. (2012) Grafting of Methanol in Dickite and Intercalation of Hexylamine. *Applied Clay Sciences*, **56**, 63-67. <https://doi.org/10.1016/j.clay.2011.11.023>
- [29] Wilson, M.J. (1994) Clay Mineralogy: Spectroscopic and Chemical Determinative Methods. Chapman & Hall, London. <https://doi.org/10.1007/978-94-011-0727-3>
- [30] Madejová, J. and Komadel, P. (2001) Baseline Studies of the Clay Minerals Society Source Clays: Infrared Methods. *Clays and Clay Minerals*, **49**, 410-432. <https://doi.org/10.1346/CCMN.2001.0490508>
- [31] Valášková, M. and Martynkova, G.S. (2012) Clay Minerals in Nature—Their Characterization, Modification and Application. IntechOpen, Rijeka.
- [32] Hattab, M., Bouziri-Adrouche, S. and Fleureau, J.M. (2010) Évolution de la Microtexture d'une Matrice Kaolinitique sur Chemin Triaxial Axisymétrique. *Canadian Geotechnical Journal*, **47**, 34-48. <https://doi.org/10.1139/T09-098>
- [33] Wu, L.M., Tong, S.D., Zhao, L.Z., Yu, W.H., Zhou, H.C. and Wang, H. (2014) Fourier Transform Infrared Spectroscopy Analysis for Hydrothermal Transformation of Microcrystalline Cellulose on Momtmorillonite. *Applied Clay Science*, **95**, 74-82. <https://doi.org/10.1016/j.clay.2014.03.014>
- [34] Colarossi, D., Duller, G.A.T., Tooth, S. and Lyons, R. (2015) Comparison of Paired Quartz OSL and Feldspar Post-IR IRSL Dose Distributions in Poorly Bleached Fluvial Sediments from South Africa. *Quaternary Geochronology*, **30**, 233-238. <https://doi.org/10.1016/j.quageo.2015.02.015>
- [35] Toussaint, F., Fripiat, J.J. and Gastuche, M.C. (1963) Dehydroxylation of Kaolinite. I. Kinetics. *Physical Chemistry*, **67**, 26-30. <https://doi.org/10.1021/j100795a007>
- [36] Manoharan, C., Dhanapandian, S., Sutharsan, P. and Venkatachalapathy, R. (2012) Characteristics of Some Clay Materials from Tamilnadu, India, and Their Possible Ceramic Uses. *Cerâmica*, **58**, 412-418. <https://doi.org/10.1590/S0366-69132012000300021>
- [37] Munvuyi, D., Ousmane, M.S. and Bougouma, M. (2022) Physicochemical and Mineralogical Characterization of Clays from the Tcheriba Zone in the Boucle of Mouhoun Region (Burkina Faso). *Journal of Materials Environment Sciences*, **13**, 755-767.
- [38] Asante-Kyei, K., Addae, A. and Aflo A. (2023) Developing Recipe from Local Ceramic Raw Materials for Making Crucibles in Ghana. *Journal of Minerals and Materials Characterization and Engineering*, **11**, 81-91. <https://doi.org/10.4236/jmmce.2023.114009>

- [39] Munvuyi, D., Ousmane M.S. and Bougouma, M. (2022) Physicochemical and Mineralogical Characterization of Clays from the Tcheriba Zone in the Boucle of Mouhoun Region (Burkina Faso). *Journal of Materials and Environmental Science*, **13**, 755-767. <http://www.jmaterenvironsci.com>
- [40] Amon, L., Konan, L., Goure-Doubi, H., Yao, J.Y., Coulibaly, J.K. and Oyetola, S. (2017) Physicochemical and Structural Properties of Clay-Based Ceramic Filters from Côte d'Ivoire. *Journal de la Société Ouest-Africaine de Chimie*, **44**, 70-77.
- [41] Huyen, D.T., Tabelin, C.B., Thuan, H.M., Dang, D.H., Truong, P.T. and Vongphuthone, B. (2019) Geological and Geochemical Characterizations of Sediments in Six Borehole Cores from the Arsenic-Contaminated Aquifer of the Mekong Delta, Vietnam. *Data in Brief*, **25**, Article ID: 104230. <https://doi.org/10.1016/j.dib.2019.104230>
- [42] Emeruwa, E., Kouadio, K.C., Kouoakou C.H., Boffoue O.M., Assande A.A., Ouatarara S., Coulibaly, Y., Dauscher, A. and Lenoir, B. (2008) Characterization of Some Clays from Abidjan Region: Comparative Study of Dispositifs and Valorisation Perspectives. *Revue Ivoirienne des Sciences et Technologie*, **11**, 177-192.
- [43] Wang, Q., Odlyha, M. and Cohen, N.S. (2000) Thermal Analyses of Selected Soil Samples from the Tombs at the Tianma-Qucun Site, Shanxi, China. *Thermochimica Acta*, **365**, 189-195. [https://doi.org/10.1016/S0040-6031\(00\)00723-1](https://doi.org/10.1016/S0040-6031(00)00723-1)
- [44] Milošević, M., Logar, M. and Biljana Djordjević, B. (2020) Mineralogical Analysis of a Clay Body from Zlakusa, Serbia, Used in the Manufacture of Traditional Pottery. *Clay Minerals*, **55**, 142-149. <https://doi.org/10.1180/clm.2020.20>